

Search for hybrid morphology radio galaxies from FIRST survey at 1400 MHz

Shobha Kumari

Midnapore City College, Kuturia, Bhadutala, West Bengal, 721129, India

and

Sabyasachi Pal

*Indian Centre for Space Physics, 43 Chalantika, Garia Station Road, 700084, India
Midnapore City College, Kuturia, Bhadutala, West Bengal, 721129, India*

ABSTRACT

Hybrid Morphology Radio Sources (HyMoRS) are a very rare and newly discovered subclass of radio galaxies that have mixed FR morphology i.e., these galaxies have FR-I structure on one side of the core and FR-II structure on the other side of the core. We systematically searched for HyMoRS using VLA Faint Images of the Radio Sky at Twenty-cm (FIRST) survey at 1400 MHz and identified forty-five confirmed HyMoRS and five candidates HyMoRS. Our finding significantly increased the known sample size of HyMoRS. HyMoRS may play an essential role in understanding the interaction of jets with the interstellar medium and a very debated topic of the FR dichotomy. We identified optical/IR counterparts for thirty-nine sources in our catalogue. In our sample of sources, five sources had Quasar-like behavior. We had estimated the spectral index and radio luminosity of HyMoR sources in our catalogue, when possible. We found that the source J1336+2329 ($\log L = 26.93 \text{ W Hz}^{-1}\text{sr}^{-1}$) was the most luminous and the source J1204+3801, a Quasar, was the farthest HyMoRS (with redshift $z=1.28$) in our sample. With the help of a large sample size of the newly discovered sources, various statistical properties were studied.

Subject headings: galaxies: active – galaxies: formation – galaxies: jets – galaxies: kinematics and dynamics – radio continuum: galaxies

1. INTRODUCTION

Radio galaxies are known to have a high mass black hole in their core ($M \sim 10^{9-12} M_{\odot}$) and two oppositely directed jets coming out of the core. Radio galaxies are classified into

two categories based on their morphology (Fanaroff & Riley 1974). FR-II galaxies are characterized by prominent hotspots at the outer edges of radio lobes with a nearly homogeneous feature. FR-I galaxies lack hotspots at the outer edges of the radio structure. It was found that most of the FR-I radio galaxies had a critical radio luminosity $L_{178MHz} < 2 \times 10^{25} \text{ W Hz}^{-1}\text{sr}^{-1}$ and that of FR-II radio galaxies, $L_{178MHz} > 2 \times 10^{25} \text{ W Hz}^{-1}\text{sr}^{-1}$ (Fanaroff & Riley 1974).

Recently, a new group of radio sources called Hybrid Morphology Radio Sources (HyMoRS) was discovered, where the radio morphology of the source exhibited both types of structures together (FR-I on one side and FR-II on the other side of the core) (Gopal-Krishna & Wiita 2000). The mixed FR morphology of HyMoRS suggests that probably these are the missing link between FR-I and FR-II radio galaxies. The FR dichotomy is a widely discussed topic for more than twenty years and the study of hybrid radio sources might be of fundamental importance to understand the origin of the FR dichotomy (Gopal-Krishna & Wiita 2000) and will give the idea that how the morphology of radio galaxies is linked to the nature of the central engine, its environment and the composition of jets? (Gopal-Krishna & Wiita 2000; de Gasperin 2017). Though the origin of HyMoRS is not completely understood, it is believed that HyMoRS is the result of the asymmetric interaction of jets with the Interstellar Medium (ISM) (Gopal-Krishna & Wiita 2000; Kapińska et al. 2017).

For the first time, Gopal-Krishna & Wiita (2000) detected six candidate HyMoRS with the help of the Giant Metrewave Radio Telescope. Using 1700 sources from the Faint Images of the Radio Sky at Twenty-cm (FIRST) survey (Becker, White & Helfand 1995), Gawroński et al. (2006) found three certain and two possible HyMoRS which proved these sources are rare. So far, a small number of HyMoRS are known and only a small fraction of them have been studied in detail. A detailed multi-wavelength radio study for two known HyMoRS (J1211+743 and J1918+742) was done by Pirya et al. (2011). Using VLBI observations Ceglowski, Gawronski & Kunert-Bajraszewska (2013) examined the five known HyMoRS with 10 kpc jet length which suggested that the origin of HyMoRS is not due to the orientation of jets as was discussed earlier (Marecki et al. 2006). Even after recent efforts to find hybrid sources, the known population of HyMoRS is still small. In the present paper, we made a systematic search for HyMoR sources using the FIRST survey (Becker, White & Helfand 1995). This paper aims to increase the known sample size of HyMoRS and thus help to understand the nature of these sources in detail, which will also be important to bridge the missing link between FR-I and FR-II radio galaxies.

The current paper was organized in the following way:

The definition of newly detected radio sources, source identification strategy, and optical counterpart identification of sources were described in Section 2. In Section 3, we elaborated

different results, in Section 4 we discussed our findings and in Section 5 we summarised the conclusions. We used the following Λ CDM cosmology parameters for the entire discussion in this paper using results from the final full-mission Planck measurements of the CMB anisotropies: $H_0 = 67.4 \text{ km s}^{-1} \text{ Mpc}^{-1}$, $\Omega_{vac} = 0.685$ and $\Omega_m = 0.315$ (Aghanim et al. 2020).

2. IDENTIFYING OF THE HYBRID MORPHOLOGY RADIO SOURCES

2.1. The VLA FIRST survey

The FIRST survey (White et al. 1997) covered a radio sky of 10,575 square degrees near the North and South Galactic caps at 1400 MHz (21 cm). This survey had a typical RMS of 0.15 mJy and an angular resolution of $5''$ (Becker, White & Helfand 1995). The FIRST survey covered approximately 25 per cent of the total sky, out of which, approximately 80 per cent was in the North Galactic cap (8,444 square degrees), and 20 per cent was in the South Galactic cap (2,131 square degrees) (Becker, White & Helfand 1995). The FIRST survey offered better resolution and sensitivity than the previous NRAO VLA Sky Survey (NVSS) at 1.4 GHz which used VLA-D configuration and covered 82 per cent of the celestial sphere with an angular resolution of $45''$ and an RMS of $\sim 0.45 \text{ mJy}$ (Condon et al. 1998). The FIRST survey used the NRAO Very Large Array (VLA) in its B-configuration (VLA-B).

With the high sensitivity and resolution of the FIRST survey, the study of the morphology of faint radio galaxies, in detail, became possible. In the last two decade, the FIRST database was used to search for radio galaxies with different distinct morphologies such as compact steep spectrum sources, core-dominated triple sources (Kunert et al. 2002; Marecki et al. 2006), giant radio sources (Kuzmicz et al. 2018), and head-tailed sources (Missaglia et al. 2019; Pal & Kumari 2021). Earlier, around seven hundred winged radio galaxy candidates were discovered with the help of the FIRST database (Cheung 2007; Yang et al. 2019; Bera et al. 2020).

2.2. Definition of hybrid morphology radio sources

HyMoRS appeared to had a mixed Fanaroff-Riley (FR) morphology, i.e., they had an FR-I type lobe on one side of its nucleus and an FR-II type lobe on the other side. These sources are very rare (<1 per cent of radio galaxies belong to this category (Gawroński et al. 2006)) and only a small number of sources was discovered previously, we aimed to increase that number by inspecting the sky covered by the VLA FIRST survey.

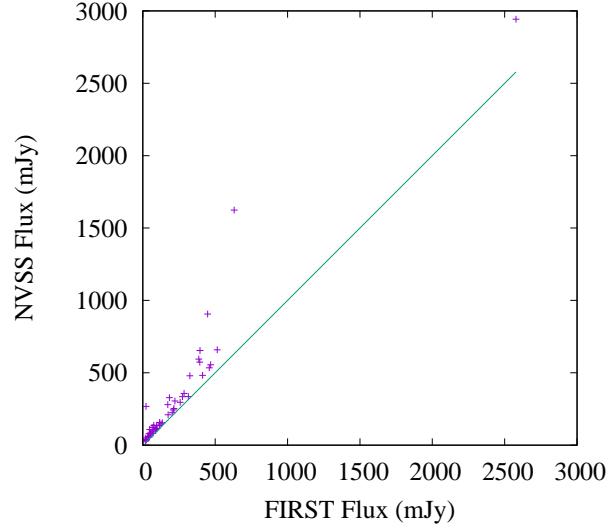


Fig. 1.— Flux densities measured from the FIRST catalogue and NVSS catalogue are shown for all HyMoRS presented in this paper

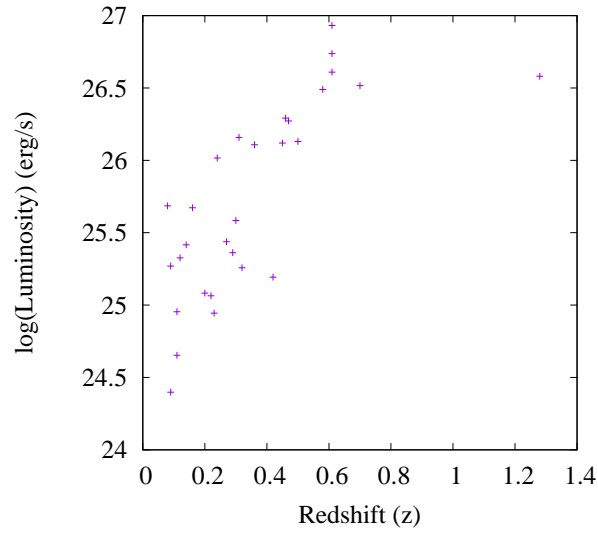


Fig. 2.— Distribution of the radio luminosity ($\log L_{rad}$) with the redshift (z) for all HyMoRS presented in this paper

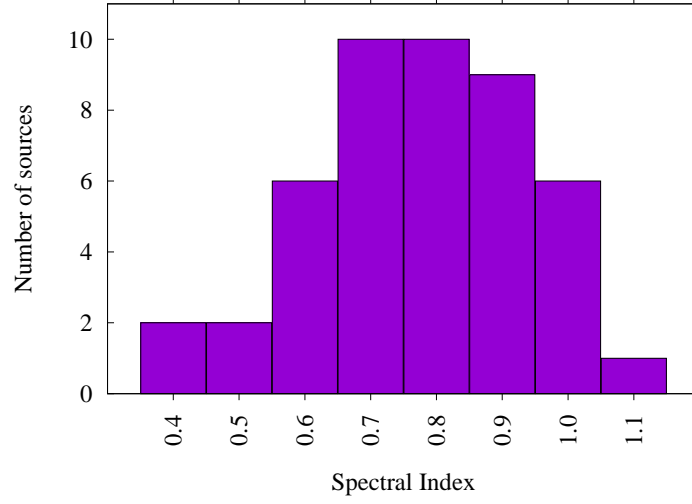


Fig. 3.— Histogram showing spectral index distribution of radio galaxies presented in the present paper for all HyMoRS.

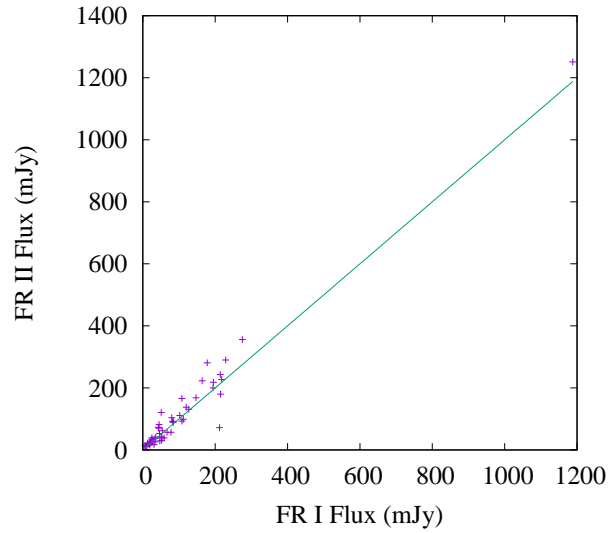
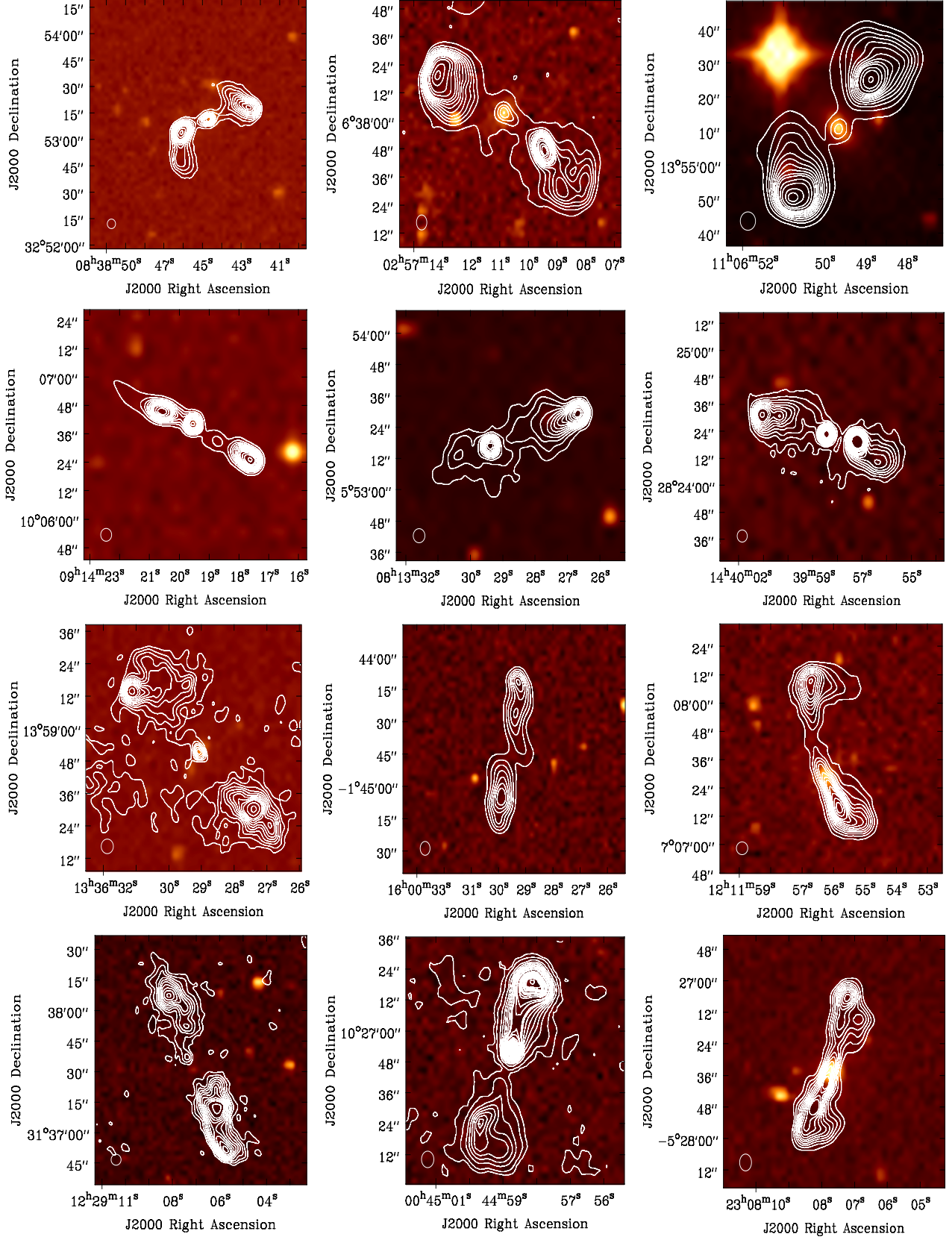


Fig. 4.— Flux densities measured for all HyMoRS of FR-I and FR-II structure

Fig. 5.— A sample of Twelve Hybrid Morphology Radio Sources (HyMoRS)



We classified HyMoRS based on the morphology of each source. We noted the brightest peak of individual jets of radio galaxies and recorded whether it was located towards the edge of the lobe or not. If the peak was located towards the edge of the lobe, we classified it as FR-II and if the location of the peak was in other places, except the edge, we classified it as FR-I. In this paper, we listed sources that had FR-I-like morphology on one side of the lobe and FR-II-like morphology on the other side.

2.3. Search strategy

We looked for radio sources whose radio structures on the two sides of the nucleus, exhibited different Fanaroff-Riley morphologies using the VLA FIRST survey. The FIRST catalogue contains a total of 946,432 radio sources. We filtered all sources in the catalogue having an angular size of $> 15''$ (i.e. at least thrice the convolution beam size). Our filtering gave an output of 20,045 sources. We visually examined the morphology of all radio sources from the fields of 20,045 sources. Through our study, we successfully discovered 45 confirmed and 5 candidates new Hybrid Morphology Radio Sources (HyMoRS). We removed two sources (J1224+0203 and J1034+2518) from our catalogue as they were listed in [Kapińska et al. \(2017\)](#).

2.4. The optical counterparts and properties

For each of the newly discovered HyMoR sources, we searched the optical/IR counterpart using the Digital Sky Survey (DSS), the Sloan Digital Sky Survey (SDSS) data catalogue ([Gunn et al. 2006](#); [Alam et al. 2015](#)) DR16¹ and NED². The identification of the optical/IR counterpart was based on the position of the optical/IR source relative to the radio galaxy morphology. DSS2 (red) optical images were overlaid with the radio images from VLA FIRST survey. The positions of the optical/IR counterparts of HyMoRS were used as the positions of these sources and were presented in the 3rd and 4th columns of Table 1. Optical/IR counterparts were found for 39 sources (26 were from the SDSS catalogue) out of a total of 50 sources. The location of the core of the radio galaxy or the intersection of both radio lobes was used as the position of the galaxies when no clear optical/IR counterparts were available.

¹<https://www.sdss.org/dr16/>

²<https://ned.ipac.caltech.edu>

3. RESULTS

3.1. Newly detected hybrid radio galaxies

We reported the discovery of a total of forty-five confirmed and five candidate HyMoRS from the VLA FIRST survey in Table 1. We identified the optical/IR counterparts of sources when available and we listed in the 5th column of Table 1 the catalogue names from where the optical counterpart was found. In the current paper, for flux density measurements, we used the NRAO VLA Sky Survey (NVSS) (Condon et al. 1998) flux densities at 1400 MHz instead of flux density measurements from FIRST and tabulated it in column 6. The FIRST survey was prone to flux density loss due to its high resolution and lack of antennas in short spacing. NVSS was better suited in detecting the most extended radio structure as the lower resolution VLA-D configuration was used for the NVSS with a resolution of $\sim 45''$ compared to the VLA-B configuration of the FIRST survey with a resolution of $\sim 5''$. In Figure 1, FIRST and NVSS flux-density distribution of all HyMoRS was shown which confirmed the flux densities from the NVSS images was significantly higher than the corresponding measurements from the FIRST images. The mean and median flux-density measurements from the NVSS catalogue were 283.7 and 136.5 mJy and the mean and median flux densities from the measurements of the FIRST catalogue were 215.6 and 115 mJy. For one source J0756+3901, we measured the 1400 MHz flux density from FIRST instead of NVSS as there was a background source in the FIRST image inside the beam size of the NVSS image.

For each source in our sample, we had calculated the corresponding flux density of the source at 150 MHz (column 7) using TGSS (Intema et al. 2017) when the source in TGSS was detected. The two-point spectral index between 1400 and 150 MHz α_{150}^{1400} was calculated when flux density at 150 MHz was available and tabulated in column 8 of Table 1. In column 9, the redshifts (z) of these sources were mentioned when available. For sources with known redshift, the luminosity of sources was tabulated in column 10. The common name of sources at radio wavelengths was listed in the last column which was mentioned earlier without identification of them as HyMoRS.

The example of twelve hybrid morphology radio galaxies was shown in Figure 5. The optical images from DSS2 (red) were overlaid with the radio images from VLA FIRST survey. Synthesized beams were shown in the lower-left corner of the images.

3.2. Spectral index (α)

The two-point spectral index of newly discovered hybrid morphology radio galaxies between 150 and 1400 MHz was calculated assuming $S \propto \nu^{-\alpha}$, where α is the spectral index and S is the radiative flux density at a given frequency ν . In Table 1, spectral index (α_{150}^{1400}) was mentioned for forty-six HyMoRS. The remaining four HyMoRS were not detectable due to low flux density in TGSS.

In Figure 3, histogram with spectral index distribution for all HyMoRS, presented in the current paper, was shown. The histogram peaks near 0.7-0.8 for these sources. Total span of α_{150}^{1400} of these sources ranged from 0.34 to 1.07. Most of the hybrid morphology radio galaxies (93.3 per cent) showed a steep radio spectrum $\alpha \geq 0.5$. The HyMoR sources J2308–0527, J0833+1028, and J0855+4911 (6.7 per cent) showed a flat spectrum ($\alpha < 0.5$). Among all HyMoRS, J1136–0328 had the highest spectral index (with $\alpha_{150}^{1400} = 1.07$) and J2308–0527 had the lowest spectral index (with $\alpha_{150}^{1400} = 0.34$). The mean and median spectral index was 0.72 and 0.73 (with 1σ standard deviation = 0.17) which was nearly equal with the spectral index of normal radio galaxies (for example, mean spectral index of 300 radio galaxies by Shimmins (1968) was 0.71).

3.3. Radio luminosity

We had calculated the radio luminosity (L_{rad}) for all the newly discovered sources (when value of z was available) using standard formula (Donoso, Best & Kauffmann 2009)

$$L_{rad} = 4\pi D_L^2 S_0 (1+z)^{\alpha-1} \quad (1)$$

where z is the redshift of the radio galaxy, α is the spectral index ($S \propto \nu^{-\alpha}$), D_L is luminosity distance to the source in metre (m), S_0 is the flux density ($\text{W m}^{-2} \text{Hz}^{-1}$) at a given frequency.

In Figure 2, we plotted the distribution of radio luminosities of HyMoRS presented in the current paper with known redshifts (z) which suggests that the most luminous HyMoR sources had redshift near about 0.6 and only one source had redshift > 1 . For sources presented in the current paper, radio luminosities at 1400 MHz are in the order of $10^{25} \text{ W Hz}^{-1} \text{sr}^{-1}$, which was similar to a typical radio galaxy (Fanaroff & Riley 1974). For FR-I, $L_{rad} < 2 \times 10^{25}$ ($\log L_{rad} = 25.3$) $\text{W Hz}^{-1} \text{sr}^{-1}$ and for FR-II, $L_{rad} > 2 \times 10^{25}$ ($\log L_{rad} = 25.3$) $\text{W Hz}^{-1} \text{sr}^{-1}$ (Fanaroff & Riley 1974). In term of luminosity sources presented in this current paper were more luminous (more powerful) than twenty-five candidates HyMoRS presented by Kapińska et al. (2017) with the help of international citizen science project, Radio Galaxy Zoo (RGZ). Because the average and median of $\log L_{rad} [\text{W Hz}^{-1} \text{sr}^{-1}]$ for HyMoRS in the current paper

were 25.7 and 25.7 respectively at $0.08 < z < 1.28$ which was close to the borderline $\log L_{rad}$ of FR-I and FR-II sources, as expected and the sources presented by Kapińska et al. (2017) had moderate power ($\log L_{rad} = 24.67 \text{ W Hz}^{-1} \text{ sr}^{-1}$) at redshifts $0.14 < z < 1.0$.

J1336+2329 was the most luminous HyMoRS in our sample with $\log L_{rad} = 26.93 \text{ W Hz}^{-1} \text{ sr}^{-1}$ ($z = 0.61$) and NVSS flux density 534 mJy. J2308–0527 was the least luminous HyMoRS in our sample with $\log L_{rad} = 24.4 \text{ W Hz}^{-1} \text{ sr}^{-1}$ ($z = 0.09$) and NVSS flux density 120 mJ

4. DISCUSSION

The origin of FR morphology in HyMoRS is still unclear. FR dichotomy is a very debated outstanding topic in astrophysics of extragalactic radio sources for more than twenty years. It is believed that the powerful FR-II structure of radio galaxies appeared due to supermassive black hole (SMBH) spin with a very high speed and if SMBH spin has a low speed then FR-I structure form (Gopal-Krishna & Wiita 2000). Bicknell (1995) proposed that the FR dichotomy results from the transition of a supersonic but relatively weak jet to a subsonic/transonic flow near the host giant galaxy’s innermost ($\sim 1 \text{ kpc}$) region due to deceleration by thermal plasma. There are more fundamental differences between FR-I and FR-II classes due to the composition of jets. For FR-I classes, $e^- - e^+$ plasma is preferred in the structure of jet while for the case of FR-II sources, $e^- - p$ could be preferred (Reynolds et al. 1996).

Here we looked for a relatively new group of radio sources called HyMoRS, where the two lobes exhibited different FR morphological types. So far, only very few HyMoRS were known (Gopal-Krishna & Wiita 2000; Gawroński et al. 2006; Kapińska et al. 2017). From a systematic search, we found 45 confirmed and 5 candidate HyMoRS from the VLA FIRST survey. Gopal-Krishna & Wiita (2000) suggested that HyMoRS may play a dominant role in the understanding of FR dichotomy and it is also in favor of some of the hypotheses in which interaction of jet power with IGM gives rise to the shape of these type of radio sources.

The redshifts were known for 31 HyMoRS out of a total of 50 sources in which twenty-six HyMoRS had spectroscopic redshift taken from SDSS and redshift of the remaining five sources were taken from NED. Five sources (i.e., J1106+1355, J0929+5157, J0044+1026, J1722+3103, J1204+3801) in our sample had Quasars like behavior. We found that the source J1204+3801, a Quasar, was the farthest HyMoRS with the highest redshift ($z = 1.28$) and the source J1254+2737 was the HyMoRS with a maximum NVSS flux density of $F_{1400} = 2943 \text{ mJy}$ amongst all sources presented in this current paper. In Figure 4, we plotted the flux

Table 1: Hybrid Morphology radio sources

Cat No.	Source name	R.A (J2000.0)	DEC (J2000.0)	Ref.	F_{1400} (mJy)	F_{150} (mJy)	α	z	Luminosity $WHz^{-1}sr^{-1} \times 10^{25}$	Common Name
1	J1118-0556	11:18:00.70	-05:56:30.0	–	82	515	0.82	–	–	–
2	J1254+2737	12:54:12.01	+27:37:33.9	SDSS	2943	10547	0.57	0.08	4.85	–
3	J0257+0638	02:57:10.96	+06:37:59.3	–	1624	7900	0.70	–	–	PKS J0257+0638
4	J1327-0249	13:27:05.73	-02:49:33.0	SDSS	595	2647	0.66	0.24	10.38	–
5	J1336+1359	13:36:29.06	+13:58:51.6	SDSS	82	324	0.61	0.22	1.16	–
6	J0838+3253	08:38:44.61	+32:53:11.8	SDSS	114	–	–	0.21	–	–
7	J1106+1355 ^α	11:06:49.67	+13:55:10.3	SDSS	555	2253	0.62	0.12	2.12	–
8	J2101+0206	21:01:10.71	+02:06:27.5	–	574	3101	0.75	–	–	4C +01.64
9	J0715+5528*	07:15:23.95	+55:28:47.1	–	107	814	0.91	–	–	–
10	J0929+5157 ^α	09:29:47.08	+51:56:55.2	–	147	1165	0.93	0.70	32.81	–
11	J1007-0454	10:07:49.30	-04:53:42.0	MRC	335	2942	0.97	0.61	54.63	PMN J1007-0453
12	J1229+3137	12:29:07.17	+31:37:31.1	SDSS	137	1009	0.89	0.50	13.48	–
13	J1156+3910	11:56:27.97	+39:10:40.3	GMBCG	27	88	0.53	0.42	1.56	–
14	J2129-0549	21:29:01.07	-05:49:50.9	2MASS	32	–	–	–	–	–
15	J1000+3959	10:00:37.09	+39:59:11.5	SDSS	55	285	0.74	–	–	–
16	J0044+1026 ^α	00:44:58.72	+10:26:53.7	GALEXASC	224	1524	0.86	0.58	30.88	–
17	J1638+3753	16:38:00.87	+37:52:59.8	2MASX	654	2617	0.62	0.16	4.70	4C +37.48
18	J1657+4319	16:57:31.94	+43:19:55.5	SDSS	104	436	0.64	0.20	1.21	–
19	J1206+2306	12:06:49.72	+23:06:17.2	SDSS	243	1614	0.85	–	–	–
20	J1722+3103 ^α	17:22:18.96	+31:03:23.8	SDSS	137	520	0.60	0.30	3.84	–
21	J0734+3507*	07:34:23.76	+35:06:42.7	–	357	1957	0.76	–	–	–
22	J0739+2451	07:39:45.33	+24:51:34.2	–	210	1157	0.76	–	–	–
23	J1027+1033	10:27:57.87	+10:33:48.6	SDSS	138	474	0.55	0.11	0.45	–
24	J1029+2954	10:29:33.80	+29:55:02.2	SDSS	253	1408	0.77	0.46	19.57	–
25	J1042+3406	10:42:28.50	+34:05:58.7	SDSS	268	1670	0.82	0.61	40.69	–
26	J1600-0144	16:00:29.60	-01:44:44.6	MRC	336	2450	0.89	–	–	PMN J1600-0144
27	J1715+2751	17:15:35.68	+27:52:10.1	VFK	80	664	0.95	–	–	–
28	J1115+2518	11:15:08.00	+25:18:44.0	–	50	343	0.86	–	–	–
29	J1211+0707	12:11:56.04	+07:07:36.3	–	155	617	0.62	–	–	–
30	J1234-0804	12:34:37.43	-08:04:14.8	2MASS	81	477	0.79	–	–	–
31	J1336+2329	13:36:23.19	+23:28:58.8	SDSS	534	4282	0.93	0.61	85.44	–
32	J1538+2144*	15:38:56.56	+21:44:57.3	SDSS	114	450	0.61	0.47	18.72	–
33	J1129+2101	11:29:24.14	+21:01:13.8	SDSS	280	958	0.55	0.11	0.90	–
34	J1204+3801 ^α	12:04:48.52	+38:01:40.1	SDSS	39	326	0.95	1.28	38.09	–
35	J0756+3901* ^β	07:56:27.36	+39:01:26.0	SDSS	172	678	0.76	0.45	13.17	–
36	J2308-0527*	23:08:07.79	-05:27:35.1	2MASS	120	254	0.34	0.09	0.25	–
37	J2147+1135	21:47:55.50	+11:35:15.0	GMBCG	83	–	–	0.36	–	–
38	J0833+1028	08:33:45.44	+10:27:53.2	WHL	93	240	0.42	0.29	2.30	–
39	J0914+1006	09:14:19.53	+10:06:40.5	SDSS	479	1896	0.61	0.31	14.39	MRC 0911+103
40	J1249+0932	12:49:25.72	+09:32:09.0	WHL	57	199	0.56	0.23	0.88	–
41	J0201+0833	02:01:23.73	+08:33:14.6	–	328	1635	0.72	–	–	PMN J0201+0832
42	J1321+0503	13:21:24.22	+05:03:43.3	SDSS	61	440	0.88	–	–	–
43	J1609+0348	16:09:24.18	+03:47:57.3	–	247	–	–	–	–	PMN J1609+0347
44	J1439+2824	14:39:58.42	+28:24:22.6	SDSS	305	1396	0.68	0.36	12.82	–
45	J0813+0553	08:13:28.90	+05:53:14.3	SDSS	136	696	0.73	–	–	–
46	J1136-0328	11:36:01.39	-03:29:13.2	MRC	296	3225	1.07	–	–	–
47	J1236+5524	12:36:47.72	+55:24:51.5	SDSS	59	182	0.50	0.32	1.81	–
48	J1435+5508	14:35:28.46	+55:07:52.0	SDSS	482	3323	0.86	0.14	2.61	–
49	J1541+4327	15:41:04.95	+43:27:02.7	SDSS	123	619	0.72	0.27	2.74	–
50	J0855+4911	08:55:56.37	+49:11:10.6	SDSS	906	2004	0.35	0.09	1.86	–

Notes–

^α –Quasars like properties.

* –FR-II flux more than FR-I flux.

^β –FIRST flux used in place of NVSS and had background source.

references–

1: NVSS (Condon et al. 1998); 2: VLSS (Cohen et al. 2007); 3: 3C (Bennett 1962; Edge et al. 1959); 4: 4C (Pilkington & Scott 1965; Gower, Scott & Wills 1967; Caswell & Crowther 1969); 5: 6C (Hales et al. 1991); 6: 7C (McGilchrist et al. 1990; Kollgaard et al. 1994; Waldram et al. 1996; Vessey & Green 1998); 7: PMN (Griffith et al. 1994); 8: PKS (Bolton, Gardner & Mackey 1964); 9: 87GB (Gregory & Condon 1991); 10: B2 (Colla et al. 1970, 1972, 1973); 11: B3 (Ficarra, Grueff & Tomassetti 1985); 12: MGC (Vorontsov-Vel’Yaminov & Arkhipova 1962); 13: WISE (Chung et al. 2011; Rebull et al. 2011); 14: NVGRC (Proctor 2016); 15: VFK (van Velzen, Falcke & Körding 2015); 16: MRC (Lloyd & Jones 2002); 17: CRATES (Healey et al. 2007); 18: FIRST (Becker, White & Helfand 1995); 19: SUMSS (Mauch et al. 2003); 20: 2MASS (Huchra et al. 2012)

density of FR-I and FR-II lobes for each HyMoRS presented in the current work. Though for most of the galaxies (87 per cent), the FR-II lobe had more flux density compared to FR-I lobe but there were five galaxies (J0715+5528, J0734+3507, J1538+2144, J0756+3901, and J2308–0527) (13 per cent) which had FR-I lobe flux density higher than that of FR-II lobe flux density. For some of them, this might be due to the fact that the flux of FR-I was boosted due to the relativistic Doppler effect. It was found that the average and median flux density of FR-I were 114 mJy and 53.5 mJy and that of FR-II were 127 mJy and 62 mJy. For twenty-six sources, including five Quasars, we found optical spectra of emission and absorption line using SDSS-DR16 (Gunn et al. 2006; Alam et al. 2015).

For five sources, J1136–0328, J1236+5524, J1435+5508, J1541+4327, and J0855+4911 presented in Table 1, they could not be conclusively classified in terms of morphology and we kept them as candidate HyMoRS. Further deep high-resolution observations are required to confirm the nature of these sources.

HyMoRS sources are very rare to find in the sky and so far only a few sources were discovered. The discovery of a good number of HyMoR sources in the current work may play a crucial role in understanding the FR-I/FR-II dichotomy and the discovery of more such objects with a future deeper survey is expected. High-resolution multi-frequency observation of these sources is encouraged to understand the nature of these sources.

5. CONCLUSIONS

We look for hybrid morphology radio sources from the VLA FIRST survey at 1400 MHz. Our main findings in this paper were as follows:

- A total of 45 confirmed and 5 candidate HyMoR sources were detected that significantly increase the number of known HyMoRS and opens up the possibility of follow-up observations of these sources with high-resolution deep radio observations. It will play a very important role in understanding the FR dichotomy.
- It was found that five of the newly discovered HyMoRS were Quasars.
- Except three sources (which showed flat spectrum) all HyMoRS showed a steep radio spectrum.
- Optical/IR counterparts were identified for 39 (26 were from SDSS) out of 50 HyMoRS (78 per cent).

ACKNOWLEDGMENTS

This research has made use of the NASA/IPAC Extragalactic Database (NED) which is operated by the Jet Propulsion Laboratory, California Institute of Technology, under contract with the National Aeronautics and Space Administration. This publication makes use of data products from the Two Micron All Sky Survey, which is a joint project of the University of Massachusetts and the Infrared Processing and Analysis Center/California Institute of Technology, funded by the National Aeronautics and Space Administration and the National Science Foundation.

REFERENCES

- Aghanim et al., 2020, A&A, 641, 67
- Alam S et al., 2015, ApJS, 219, 12
- Becker R. H., White R. L., Helfand D. J., 1995, ApJ, 450, 559
- Bennett A. S., 1962, MmRAS, 68, 163
- Bera S., Pal S., Sasmal T. K., Mondal S., 2020, ApJS, 251, 9
- Bicknell G. V., 1995, ApJS, 101, 29
- Bolton J. G., Gardner F. F., Mackey M. B., 1964, AuJPh, 17, 340
- Caswell J. L., Crowther J. H., 1969, MNRAS, 145, 181
- Cegłowski M., Gawronski M. P., Kunert-Bajraszewska M., 2013, A&A, 557, A75
- Cheung C. C., 2007, AJ, 133, 2097
- Chung S M., Eisenhardt P R., Gonzalez A H., Stanford S A., Brodwin M., Stern D., Jarrett T., 2011, ApJ, 743, 34
- Cohen A. S., Lane W. M., Cotton W. D., Kassim N. E., Lazio T. J. W., Perley R. A., Condon J. J., Erickson W. C., 2007, AJ, 134, 1245
- Colla G et al., 1970, A&AS, 1, 281
- Colla G et al., 1972, A&AS, 7, 1
- Colla G., 1973, A&AS, 11, 291

- Condon J. J., Cotton W. D., Greisen E. W., Yin Q. F., Perley R. A., Taylor G. B., Broderick J. J., 1998, *AJ*, 115, 1693
- de Gasperin F., 2017 *MNRAS*, 467, 2234
- Donoso E., Best P. N., Kauffmann G., 2009, *MNRAS*, 392, 617
- Edge D. O., Shakeshaft J. R., McAdam W. B., Baldwin J. E., Archer S., 1959, *MmRAS*, 68, 37
- Fanaroff B. L., Riley J. M., 1974, *MNRAS*, 167, 31P
- Ficarra A., Gruett G., Tomassetti G., 1985, *A&AS*, 59, 255
- Gawroński M. P., Marecki A., Kunert-Bajraszewska M., Kus A. J., 2006, *A&A*, 447, 63
- Gopal-Krishna, Wiita P. J., 2000, *A&A*, 363, 507
- Gower J. F. R., Scott P. F., Wills D., 1967, *MmRAS*, 71, 49
- Gregory P. C., Condon J. J., 1991, *ApJS*, 75, 1011
- Griffith M. R., Wright A. E., Burke B. F., Ekers R. D., 1994, *ApJS*, 90, 179
- Gunn J. E et al., 2006, *AJ*, 131, 2332
- Hales S. E. G., Mayer C. J., Warner P. J., Baldwin J. E., 1991, *MNRAS*, 251, 46
- Healey S. E., Romani R. W., Taylor G. B., Sadler E. M., Ricci R., Murphy T., Ulvestad J. S., Winn J. N., 2007, *ApJS*, 171, 61
- Huchra J. P et al., 2012, *ApJS*, 199, 26
- Intema H. T., Jagannathan P., Mooley K. P., Frail D. A., 2017, *A&A*, 598, A78
- Lloyd B. D., Jones P. A., 2002, *MNRAS*, 331, 717L
- Kapińska A. D et al., 2017, *AJ*, 154, 16
- Kollgaard R. I., Brinkmann W., Chester M. M., Feigelson E. D., Hertz P., Reich P., Wielebinski R., 1994, *ApJS*, 93, 145
- Kunert M., Marecki A., Spencer R. E., Kus A. J., Niezgoda J., 2002, *A&A*, 391, 47
- Kuźmich A., Jamroz M., Bronarska K., Janda-Boczar K., Saikia D. J., 2018, *ApJS*, 238, 9

- Marecki A., Thomasson P., Mack K. H., Kunert-Bajraszewska M., 2006, *A&A*, 448, 479
- Mauch T., Murphy T., Buttery H. J., Curran J., Hunstead R. W., Piestrzynski B., Robertson J. G., Sadler E. M., 2003, *MNRAS*, 342, 1117
- McGilchrist M. M., Baldwin J. E., Riley J. M., Titterington D. J., Waldram E. M., Warner P. J., 1990, *MNRAS*, 246, 110
- Miller B. P., Brandt W. N., 2009, *AJ*, 26
- Missaglia V., Massaro F., Capetti A., Paolillo M., Kraft R. P., Baldi R. D., Paggi A., 2019, *A&A*, 626, A8
- Pal S., Kumari S., 2021, arXiv:2103.15199
- Peacock J. A., 1983, *MNRAS*, 202, 615
- Pilkington J. D. H., Scott J. F., 1965, *MmRAS*, 69, 183
- Pirya A., Nandi S., Saikia D. J., Singh M., 2011, *BASI*, 39, 547
- Proctor D. D., 2016, *ApJS*, 224, 18
- Rebull L. M et al., 2011, *ApJS*, 196, 4
- Reynolds C. S., Fabian A. C., Celotti A., Rees M. J., 1996, *MNRAS*, 283, 873
- Smirnov N., 1948, *Ann. Math. Stat.*, 19, 279
- Shimmins A. J., 1968, *ApL*, 2, 157
- van Velzen S., Falcke H., Körding E., 2015, *MNRAS*, 446, 2985
- Vessey S. J., Green D. A., 1998, *MNRAS*, 294, 607
- Vorontsov-Vel’Yaminov B. A., Arkhipova V. P., 1962, *Morphological Trudy Gos. Astron. Inst. Shternberga*, 1
- Wall J. V., 1980, *Royal Society of London Philosophical Transactions Series A*, 296, 367
- Wall J. V., Pearson T. J., Longair M. S., 1980, *MNRAS*, 193, 683
- Waldram E. M., Yates J. A., Riley J. M., Warner P. J., 1996, *MNRAS*, 282, 779
- White R. L., Becker R. H., Helfand D. J., Gregg M. D., 1997, *ApJ*, 475, 479

Yang X et al., 2019, ApJS, 245, 17